

Tuning Magnetic Properties in Bi-2212 via Praseodymium Substitution

Hasan Ağıl^{1*} , Hicran Kurt² , Hakan Gündoğmuş³ 

¹Hakkari University, Department of Material Science and Engineering, Faculty of Engineering, Hakkari, Türkiye, hasanagil@hakkari.edu.tr, ror.org/00nddb461

²Hakkari University, Department of Physics, Graduate Education Institute, Hakkari, Türkiye, hicrankurt30@gmail.com, ror.org/00nddb461

³Hakkari University, Department of Mechanical Engineering, Faculty of Engineering, Hakkari, Türkiye, hakangundogmus@hakkari.edu.tr, ror.org/00nddb461

*Corresponding Author

ARTICLE INFO

ABSTRACT

Keywords:

Sol-gel synthesis
Curie-Weiss law
Magnetic susceptibility
Curie constant
Effective magnetic moment



Article History:

Received: 07.09.2025

Revised: 25.10.2025

Accepted: 08.12.2025

Online Available: 28.01.2026

The present study investigates the magnetic behavior of Pr-doped $\text{Bi}_2\text{Sr}_2\text{CaCu}_2\text{O}_{8+\delta}$ (Bi-2212) ceramics synthesized via the sol-gel method, focusing on how Pr substitution alters their paramagnetic response. Magnetic susceptibility ($M-T$), inverse susceptibility ($1/\chi-T$), derivative ($dM/dT-T$), and magnetization-field ($M-H$) measurements were conducted for samples with doping levels $x = 0.1, 0.2,$ and 0.3 . Linear fitting of the $1/\chi-T$ curves enabled the determination of the Curie constant (C), effective magnetic moment (μ_{eff}), and Curie-Weiss temperature (θ_{CW}). All samples exhibited positive θ_{CW} values, indicating weak ferromagnetic correlations without the formation of long-range magnetic order. Increasing Pr concentration led to systematic reductions in both C and μ_{eff} , suggesting damping of the Pr magnetic moments and suppression of superconductivity. $M-H$ measurements further confirmed a linear, hysteresis-free paramagnetic response across all compositions. This study provides a systematic experimental evaluation of how Pr substitution alters key magnetic parameters—such as the Curie constant, effective magnetic moment, and Curie-Weiss temperature—in Bi-2212 ceramics, offering an original contribution to understanding the paramagnetic transition behavior in Pr-doped high- T_c systems. Overall, the results demonstrate that Pr incorporation effectively tunes the magnetic characteristics of Bi-2212 and induces a transition toward enhanced paramagnetic behavior.

1. Introduction

High-temperature superconductors (HTS), especially the $\text{Bi}_2\text{Sr}_2\text{CaCu}_2\text{O}_{8+\delta}$ (Bi-2212) compound, are of great interest in both fundamental research and applied technologies due to their high critical temperatures and current carrying capacities [1]. The magnetic properties of Bi-2212, particularly its paramagnetic behavior and compliance with the Curie-Weiss law, are closely linked to the material's microstructural properties and the presence of doping elements [2].

Doping with rare earth elements stands out as an effective method to modulate the magnetic properties of Bi-2212. In particular, praseodymium (Pr) doping can significantly affect the paramagnetic properties of the material by effects such as suppression of magnetic moments and modification of spin-spin interactions [3]. The impact of such doping on parameters such as the Curie constant (C), effective magnetic moment (μ_{eff}), and Curie-Weiss temperature (θ_{CW}) have been investigated in various studies in the literature [4, 5]. In Bi-2212, Pr^{3+} ions preferentially substitute Ca^{2+} sites located between the CuO_2 planes, which effectively alter the hole concentration and local

spin interactions in the superconducting layers. This Ca-site substitution is known to suppress superconductivity and enhance paramagnetic behavior [5, 6].

Magnetic susceptibility (χ) and reverse susceptibility ($1/\chi$) measurements are fundamental tools for understanding the magnetic behavior of materials. The data obtained from these measurements are analyzed within the framework of the Curie–Weiss law, providing information about the magnetic interactions and moment-carrying capacity of the material [7]. Additionally, dM/dT – T curves and M – H hysteresis measurements are used to reveal magnetic phase transitions and field-dependent magnetization behavior [8]. It should be noted that pristine Bi-2212 is a high- T_c superconductor; however, Pr substitution suppresses its superconductivity and induces localized magnetic moments, resulting in a transition from superconducting to paramagnetic behavior. This transformation has been reported in earlier studies on rare-earth-doped Bi-based cuprates [2, 6].

Several studies have shown that Pr doping in Bi-based cuprates modifies both the structural and magnetic properties, leading to reduced hole concentration and suppression of T_c [5, 6, 9]. Moreover, anisotropic magnetic behavior and enhanced paramagnetic response have been observed in rare-earth-containing layered oxides [10]. These findings highlight the critical role of rare-earth substitution in controlling the balance between superconductivity and magnetism in Bi-2212 systems, providing a strong motivation for the present investigation.

In this study, the magnetic properties of Pr-doped $\text{Bi}_2\text{Sr}_2\text{CaCu}_2\text{O}_{8+\delta}$ (Bi-2212) ceramics synthesized by the sol-gel method were systematically investigated. Although previous studies have reported the suppression of superconductivity and emergence of paramagnetism in Pr-doped Bi-based systems [5, 6, 9], a comprehensive and quantitative analysis of how Pr substitution modifies key magnetic parameters has not been presented in detail. Therefore, this work aims to elucidate the correlation between Pr doping ratio and magnetic characteristics—such as Curie constant (C),

effective magnetic moment (μ_{eff}), and Curie–Weiss temperature (θ_{CW})—to provide new insight into the evolution from superconducting to paramagnetic behavior in Bi-2212 systems.

2. General Methods

$\text{Bi}_2\text{Sr}_2\text{Ca}_{1-x}\text{Pr}_x\text{Cu}_2\text{O}_{8+\delta}$ ($x = 0.1, 0.2, 0.3$) ceramics were synthesized using the sol-gel method. Analytical grade $\text{Bi}(\text{NO}_3)_3 \cdot 5\text{H}_2\text{O}$, $\text{Sr}(\text{NO}_3)_2$, Pr_6O_{11} , $\text{Ca}(\text{NO}_3)_2 \cdot 4\text{H}_2\text{O}$, and $\text{Cu}(\text{NO}_3)_2 \cdot 3\text{H}_2\text{O}$ (99% purity) were used as starting precursors. The required amounts of each reagent were calculated stoichiometrically according to the nominal formula $\text{Bi}_2\text{Sr}_2\text{Ca}_{1-x}\text{Pr}_x\text{Cu}_2\text{O}_{8+\delta}$, where x represents the substitution ratio of Pr^{3+} for Ca^{2+} . Thus, the doping levels $x = 0.1, 0.2$, and 0.3 correspond to 10%, 20%, and 30% Pr replacement at the Ca site, representing low, medium, and high substitution levels, respectively. Each nitrate salt was dissolved separately in a mixed solvent of distilled water, nitric acid, and diethylene glycol to ensure complete homogenization, followed by gelation through controlled heating. The obtained gel was dried, ground, and calcined at $750\text{ }^\circ\text{C}$ for 12 h to remove residual organics. The resulting powder was then re-ground, pelletized under 4 tons of pressure, and sintered at $860\text{ }^\circ\text{C}$ for 60 h, followed by a post-annealing step at $800\text{ }^\circ\text{C}$ for 12 h. The final samples are referred to as sample B ($x = 0.1$), sample C ($x = 0.2$), and sample D ($x = 0.3$).

In this study, Pr^{3+} ions were intended to substitute Ca^{2+} sites located between the CuO_2 planes in the Bi-2212 crystal structure. This site was selected because Ca-site substitution effectively alters the charge carrier concentration and spin interactions within the CuO_2 layers, leading to a more pronounced paramagnetic behavior. Previous studies have reported that Pr substitution at Ca sites strongly suppresses superconductivity in Bi-2212 by reducing hole concentration in the CuO_2 planes [5, 6]. Although Sr-site substitution has also been observed under certain synthesis conditions [9], the stoichiometry and synthesis route used in this work specifically aim at Ca-site occupancy.

Magnetic susceptibility (χ) is a quantitative measure of a material's response to an external magnetic field and is defined as:

$$\chi = \frac{M}{H} \quad (1)$$

where M is the magnetization per unit volume (emu/cm^3), and H is the applied external magnetic field (Oe or A/m) and is kept constant in the experiment.

The χ - T curve used in this study was obtained from the M - T (magnetization-temperature) data measured under a constant magnetic field. For all samples, the applied external field was fixed at 1000 Oe, and the temperature was scanned between 10 K and 300 K. Therefore:

$$\chi(T) = \frac{M(T)}{H} \quad (2)$$

According to Eq. (2), the magnetic susceptibility was calculated by dividing the measured magnetization value by $H = 1000$ Oe for each temperature. The obtained χ - T curves were used to analyze the magnitude of the paramagnetic response and its temperature-dependent change, depending on the doping ratio.

The $1/\chi - T$ graph was obtained by taking the inverse of the susceptibility values calculated using Eq. (1). This graph is prepared to evaluate compliance with the Curie or Curie-Weiss law, which is widely used, especially in the analysis of paramagnetic materials. Plotting the inverse susceptibility against temperature on the temperature axis on the graph shows that the system:

- To verify its paramagnetic character,
- Calculate the effective magnetic moment (μ_{eff}) concerning the Curie constant (C) or the slope of the curve,
- Determine the Curie-Weiss temperature (θ) from the point where the curve intersects the axis.

Within the scope of magnetic characterization studies, magnetization-temperature (M - T) data of the samples were collected under a constant magnetic field ($H = 1000$ Oe) in the temperature range of 10-300 K. These data were derived to

create a dM/dT curve to analyze the magnetic response of the system to temperature in more detail.

For this purpose, the first derivative of the magnetization concerning temperature for each temperature point in the M - T data was calculated numerically as follows:

$$\frac{dM}{dT} \approx \frac{M_{i+1} - M_i}{T_{i+1} - T_i} \quad (3)$$

The $dM/dT - T$ curve obtained here provides essential information, especially in the following aspects:

- Detection of magnetic transitions: Abrupt changes in the dM/dT curve, zero crossings, or maximum and minimum points provide clues for detecting possible magnetic phase transitions (e.g., Curie point, spin order, superconducting transition).
- Change in magnetic sensitivity with temperature: The dM/dT value indicates the sensitivity of the system's magnetization response to temperature. A high dM/dT value means that the magnetization changes rapidly with temperature.
- Parasitic phases or structural irregularities: Sudden distortions in the curve or second derivative signals may indicate inhomogeneous magnetic distributions or secondary phases within the sample.
- Signs of superconductivity: In samples containing a superconducting phase, a sharp change in the slope of the dM/dT curve is expected around the transition temperature (T_c). In this study, such a break of slope was not observed due to the suppression of superconductivity by Pr doping.

All magnetic measurements were conducted using a Vibrating Sample Magnetometer (VSM) module attached to a Quantum Design Physical Property Measurement System (PPMS). The M - T (magnetization-temperature) data were collected under a constant magnetic field of 1000 Oe within the temperature range of 10-300 K, while the M - H (magnetization-field) data were obtained at 10 K in the magnetic field range of ± 7 T. The inverse magnetic susceptibility ($1/\chi$ - T) curves were derived from the experimental M -

T data by taking the reciprocal of $\chi = M/H$. The $dM/dT-T$ curves were obtained numerically by applying a finite-difference derivative method to the $M-T$ dataset. No smoothing, interpolation, or functional fitting was applied; the results represent raw experimental data within the instrument's sensitivity limits.

2.1. Curie constant (C) and effective magnetic moment (μ_{eff})

The procedures used to determine the Curie constant and effective magnetic moment of samples are detailed below.

- i. First, χ was calculated from the $M-T$ data, as previously explained above.
- ii. Then, the inverse of the susceptibility was taken, and the $1/\chi-T$ graph was created.
- iii. According to Curie's law for paramagnetic systems:

$$\chi = \frac{C}{T} \Rightarrow \frac{1}{\chi} = \frac{T}{C} \quad (4)$$

Therefore, the $1/\chi$ values corresponding to the temperature were calculated, and the $1/\chi-T$ graph was obtained.

- iv. When the $1/\chi-T$ curve (see Fig. 1b) was examined, it was observed that the data was linear in the range of approximately 50–150 K. Linear regression was applied using the temperature and $1/\chi$ data in this region.
- v. Slope (m) was calculated by linear regression:

$$\frac{1}{\chi} = mT + b \quad (5)$$

Since the slope (m) as a result of the regression is equal to $1/C$, the Curie constant was determined by taking $C = 1/m$.

- vi. The effective magnetic moment was calculated from the Curie constant with the following equation:

$$\mu_{eff} = \sqrt{8C} \quad (6)$$

- vii. Finally, it is worth noting that this method is valid within the temperature range where the system complies with the Curie law.

2.2. Curie-Weiss temperature (θ_{CW})

The Curie-Weiss temperature (θ_{CW}) is obtained from the point where the line applied to the linear region between the reverse magnetic susceptibility ($1/\chi$) and the temperature (T) intersects the T-axis. The Curie-Weiss law is characterized by the Eq. (7):

$$\chi(T) = \frac{C}{T-\theta_{CW}} \Rightarrow \frac{1}{\chi} = \frac{T-\theta_{CW}}{C} \quad (7)$$

where C is the Curie constant. According to this equation, the value at which the straight line cuts the T-axis on the $1/\chi-T$ graph is θ_{CW} .

In the previous steps, we performed direct linear regressions on the $1/\chi-T$ data, and the θ_{CW} for each sample can be obtained using Eq. (8).

$$\frac{1}{\chi} = mT + b \Rightarrow \theta_{CW} = -\frac{b}{m} \quad (8)$$

3. Results and Discussion

The following analyses are based on experimental magnetization data obtained from VSM measurements. The $\chi-T$, $1/\chi-T$, $dM/dT-T$, and $M-H$ curves discussed below were derived directly from the measured $M-T$ and $M-H$ datasets of each sample.

As demonstrated in Fig. 1a, which presents the temperature-dependent change in magnetic susceptibility of sample B, it is evident that the $\chi(T)$ value exhibits a monotonic decrease within the temperature range of 10–300 K. The obtained curve is indicative of a typical paramagnetic response. It is particularly evident at low temperatures (10–60 K), where the susceptibility exhibits elevated values. Conversely, as the temperature rises, the χ value declines precipitously, attaining a virtually saturated level of approximately 300 K. This phenomenon follows the classical Curie law ($\chi=C/T$). No diamagnetic response is observed for the superconducting transition.

This finding suggests that when Pr doping is integrated into the superconducting Bi-2212 matrix, it enhances the effectiveness of Pr^{3+} ions carrying magnetic moments within the system. Consequently, the superconducting phase is suppressed. In addition, a significant body of

research in the relevant literature has reported that with increasing Pr doping, the superconductivity in the Bi-2212 system weakens, and the local magnetic moments become dominant in the paramagnetic behavior [5, 9, 11].

The present study contributes to this understanding by providing quantitative magnetic analysis of how Pr incorporation affects superconductivity in Bi-2212. While earlier works primarily demonstrated the suppression of superconductivity through resistivity or magnetization onset measurements [5, 6, 9], the current work systematically correlates the increase in Pr concentration with measurable changes in Curie constant (C), effective magnetic moment (μ_{eff}), and Curie–Weiss temperature (θ_{CW}). These parameters collectively reveal that Pr doping not only weakens the superconducting phase but also promotes short-range magnetic correlations and localized spin formation, which dominate the overall magnetic response.

Consequently, the χ - T curve observed in sample B demonstrates that the system transitions to a fully paramagnetic state, and Pr doping disrupts the structural and magnetic continuity of the superconducting phase, thereby eradicating the phenomenon of superconductivity.

As demonstrated in Fig. 1b, the $1/\chi - T$ plot was prepared with the objective of verifying the paramagnetic character of sample B. The graph generally shows that the reverse susceptibility increases linearly with increasing temperature. This phenomenon can be interpreted as a paramagnetic response governed by Curie's law, which states that the magnetic susceptibility of a substance is directly proportional to its temperature. It is noteworthy that the region of observation, which exhibits a nearly linear relationship between 50 and 200 K, indicates that the system displays classical paramagnetic behavior within this temperature range.

However, the slight deviation of the curve after 200 K (departure from linearity) indicates that weak spin-spin interactions or minor structural distortions may be effective between the ions carrying the magnetic moment. Such deviations

have been associated in the literature with magnetic disorder, local phase separations, or inhomogeneous distribution of the magnetic field within the sample [12].

The fact that the linear region intersects the positive temperature axis shows that the system can also be described by the Curie–Weiss law $\chi = C/(T - \theta)$. If we assume that the graph intersects the axis at a point close to zero, the Curie–Weiss temperature (θ) is approximately 0 K. This indicates that the magnetic spin-spin interaction in the sample is very weak, and the Pr^{3+} ions behave as isolated paramagnetic centers in the system [13].

These observations suggest that Pr doping suppresses superconductivity and leads to the development of a paramagnetic phase, but this phase does not tend to form a magnetic order. This is consistent with studies in the literature, which show that Pr doping increases the local moment effect in the Bi-2212 system but does not induce long-range magnetic order [6, 10].

The $dM/dT - T$ curve of sample B, shown in Fig. 1c, was created by differentiating the $M - T$ data obtained under a constant magnetic field. The curve generally shows negative values, and it is observed that the dM/dT value approaches zero as the temperature increases. This indicates that the rate of change in magnetization decreases with increasing temperature, and the system progresses toward saturation with a paramagnetic character.

In the low-temperature region (10–50 K), the dM/dT value reaches high negative values, such as $-0.25 \times 10^{-3} \text{ emu/cm}^3 \text{ K}$, indicating that the system responds to temperature with high magnetic susceptibility and that the local magnetic moments of Pr^{3+} ions are pretty active. The high slope in this region is a reflection of the typical Curie paramagnetic behavior observed in Pr-doped Bi-2212 systems in the literature [13].

As the temperature increases (after about 100 K), the slope of the curve gradually decreases and reaches $dM/dT \approx 0$ at temperatures above 250 K. This indicates that the system no longer exhibits a significant change in the magnetization value, i.e., it has reached a thermodynamically stable

paramagnetic state. This behavior is typical of the temperature-proportional resolution of magnetic moments, which, together with the compliance with Curie's law, explains [13].

All magnetization measurements were carried out experimentally using a vibrating sample magnetometer (VSM, Quantum Design PPMS platform). The temperature-dependent magnetization ($M-T$) data were obtained in the range of 10–300 K under a constant magnetic field of 1000 Oe, while the field-dependent magnetization ($M-H$) measurements were performed at 10 K in the field range of ± 7 T. These datasets form the basis of the $\chi-T$, $1/\chi-T$, $dM/dT-T$, and $M-H$ analyses presented in the Results section.

In addition, the absence of any sharp jumps, minimums, maximums, or zero crossing points in the graph indicates that there is neither a superconducting transition (T_c) nor a ferro- or antiferromagnetic phase transition in the system. This finding confirms that superconductivity is completely suppressed due to Pr doping, and the system exhibits paramagnetic properties alone [6].

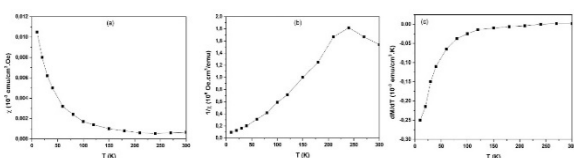


Figure 1. (a) Temperature-dependent magnetic susceptibility ($\chi-T$), (b) inverse magnetic susceptibility ($1/\chi-T$), and (c) magnetization versus temperature ($dM/dT-T$) curves of sample B

The results for sample B ($x = 0.1$) are shown here as a representative example of the magnetic response and analytical approach. The corresponding analyses for samples C ($x = 0.2$) and D ($x = 0.3$) are presented in Figures 2 and 3, respectively.

To further verify the paramagnetic behavior identified in the $\chi-T$ and $dM/dT-T$ curves of sample B, inverse susceptibility ($1/\chi-T$) analyses were extended to all compositions. This comparison provides a quantitative evaluation of how the Curie constant and effective magnetic moment evolve with increasing Pr concentration.

Fig. 2a shows the $1/\chi-T$ data of sample B, along with the linear regression results applied to these data between 50 and 150 K. The Curie constant and effective magnetic moment values of the samples determined using this approach are given in Table 1.

The values obtained for sample B clearly show that, after Pr doping, the sample completely lost its superconductivity and acquired a paramagnetic character. However, it is noteworthy that the calculated effective magnetic moment is relatively low. $\mu_{eff} \approx 0.030 \mu_B$, which is very small compared to the theoretical magnetic moment of an ideal Pr^{3+} ion (3.58–3.6 μ_B). This indicates that the magnetic moments are either not localized or only a portion of the Pr ions make a magnetic contribution. It also suggests that the moments are damped by interaction with the superconducting matrix or that some of the Pr ions are located in non-magnetic phases.

As a result, the Curie constant C confirms that the magnetic susceptibility of the system decreases with temperature in a classical paramagnetic manner. The effective magnetic moment μ_{eff} indicates that there are weak local magnetic moments in the system, and no strong spin-spin interactions are present. Pr doping suppressed superconductivity, but no magnetic ordering or high moment formation was observed.

From a microscopic perspective, the decrease in μ_{eff} with increasing Pr concentration can be explained by enhanced hybridization between the Pr^{3+} 4f orbitals and the O 2p states in the CuO_2 planes. This hybridization promotes partial delocalization of the 4f electrons and leads to the quenching of the localized Pr magnetic moments. In addition, strong Pr–O–Cu superexchange interactions can modify the spin correlations between Cu^{2+} ions and Pr^{3+} centers, further weakening the net magnetic response. These combined effects result in the systematic reduction of μ_{eff} and the dominance of short-range magnetic correlations at higher Pr contents.

The linear trend in the temperature-dependent reverse magnetic susceptibility ($1/\chi-T$) data for sample C in Fig. 2b in the range of 50–150 K reveals that the system exhibits classical

paramagnetic behavior under the Curie law. The Curie constant and effective magnetic moment values calculated according to the slope value obtained from the linear regression analysis applied to this linear region are given in Table 1. The very low effective magnetic moment suggests that the magnetic moment of the Pr^{3+} ions in the system is largely suppressed, indicating that only a limited number of Pr ions are magnetically active.

According to the literature, the effective magnetic moment of an ideal Pr^{3+} ion is theoretically approximately $3.58 \mu_B$ [14]. However, it has been previously reported by J.L. Tallon et al. [13] that Pr doping suppresses superconductivity in the Bi-2212 system while simultaneously not creating magnetic ordering but rather remaining in the form of single local moments. This low μ_{eff} value observed in sample C is in good agreement with this literature.

This also indicates that although the magnetic centers in the system increase as the doping rate increases, the moments do not correlate with each other, and the magnetic interaction remains short-range. Thus, superconductivity was suppressed entirely by Pr doping, but it was replaced by a weak paramagnetic response, not a ferromagnetic or antiferromagnetic ordering.

When the temperature-dependent reverse magnetic susceptibility ($1/\chi-T$) of sample D is examined in Fig. 2c, a strong linear relationship is observed in the range of 50–150 K. This linear region indicates that the system exhibits a classical paramagnetic response, following the Curie law ($\chi = C/T$). The Curie constant and effective magnetic moment values calculated using the slope value obtained from linear regression applied to this curve are presented in Table 1.

The estimated μ_{eff} value confirms the existence of magnetic moment-carrying centers (especially Pr^{3+} ions) in the system but also indicates that these moments are suppressed or neutralized to a significant extent. This experimentally obtained low μ_{eff} value indicates that the system does not exhibit any long-range magnetic ordering (ferro- or antiferromagnetic) despite being magnetically active. This also suggests that some of the Pr ions

are localized in non-magnetic phases or their spin moments are damped in the superconducting matrix [14, 15]

These findings were similarly reported in previous studies by J.L. Tallon et al. [13]. Although the Pr doping suppresses superconductivity, the system exhibits only weak paramagnetic character, suggesting that the doping neutralizes not only the carrier density but also the interaction of magnetic moments.

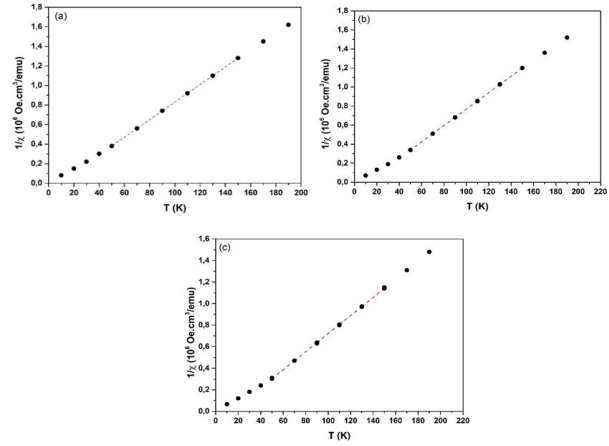


Figure 2. $1/\chi-T$ data and the linear regression results of samples (a) B, (b) C, and (c) D. Black dots are raw $1/\chi$ data, and red dashed lines are linear regression results in the 50–150 K range

Table 1. Curie constant (C) and effective magnetic moment (μ_{eff}). The effective magnetic moment is given in terms of Bohr magnetons

Sample	C (emu.K/cm ³ .Oe)	μ_{eff} (μ_B)	θ_{CW} (K)
B	1.11×10^{-4}	≈ 0.030	≈ 53.85
C	1.07×10^{-4}	≈ 0.029	≈ 50.21
D	1.03×10^{-4}	≈ 0.028	≈ 44.65

In this study, Curie-Weiss temperatures (θ_{CW}) were calculated using linear regression analyses performed on the reverse magnetic susceptibility ($1/\chi$) versus temperature (T) data of Pr-doped $\text{Bi}_2\text{Sr}_2\text{Ca}_{1-x}\text{Pr}_x\text{Cu}_2\text{O}_{8+\delta}$ ($x = 0.1, 0.2, 0.3$) samples, and are presented in Table 1.

The fact that all the obtained temperature values are positive indicates that the doped systems exhibit dominant ferromagnetic correlations in the low-temperature region. However, these ferromagnetic correlations are not strong enough to produce long-range magnetic order; the system generally continues to exhibit paramagnetic properties.

Positive θ_{CW} values have also been reported in some studies on similar structures. The magnetic effect of rare-earth doping in the Bi-2212 system was studied by Lee et al., who stated that the positive Curie-Weiss temperatures are based on spin-spin correlations [2].

In this context, the decrease in the θ_{CW} value as the doping ratio increases indicates that the ferromagnetic correlations in the system are weakened, and the magnetic interactions are increasingly suppressed. This suggests that Pr doping affects not only the carrier density but also the spin-level interactions, creating magnetic distortion and moment quenching. This trend is also consistent with the decreasing effective magnetic moment values.

$M-H$ (Magnetization–Magnetic Field) curves are a powerful tool, especially for determining the behavior and characteristic parameters of magnetic materials. Different information can be obtained from these curves for both superconducting and paramagnetic systems. Table 2 details the main parameters that can be determined from the $M-H$ curves for Pr-doped Bi-2212 derivatives.

Table 2. Parameters that can be determined from $M-H$ Curves

Parameter	Explanation
Remanent Magnetization (M_r)	The remaining magnetization in the system when $H = 0$. Only if there is a magnetic order; in paramagnetic systems, it is usually approximately zero.
Coercive Field (H_c)	The value of the reverse field at the point where $M = 0$. It is significant in ferro/antiferromagnetic or superparamagnetic systems. It is minimal in paramagnetic systems.
Maximum magnetization (M_{max})	Saturation magnetization at maximum applied H field. In paramagnetic systems, saturation does not occur, resulting in a linear response.
Magnetic permeability (μ)	Slope $(dM/dH) = \chi$ (magnetic susceptibility). Derived from the slope at the beginning of the field.

While the $1/\chi-T$ analysis confirms the paramagnetic nature of all samples, the $M-H$ measurements provide a complementary view by examining how the magnetization responds to the applied magnetic field. These field-dependent curves offer additional insight into the magnetic reversibility and the absence of long-range ordering in Pr-doped Bi-2212. The parameters given in Table 2 were determined from the $M-H$ curves of the samples. In Fig. 3a, the $M-H$ curve of sample B exhibits a typical paramagnetic behavior with a linear and hysteresis-free character up to $H = \pm 7$ T. The absence of coercive field and remanent magnetization indicates that the system does not contain any ferromagnetic or antiferromagnetic ordering, and the magnetic moments are aligned linearly and reversibly with the applied field. This finding is also consistent with the Curie-type behavior obtained from the $M-T$ curves. At the highest applied field, around ~ 7 T, M_{max} is ≈ 3.2 emu/g. However, it should be noted that the curve has not yet reached saturation, a typical feature of paramagnetic systems.

In Fig. 3b, the $M-H$ curve of sample C exhibits a symmetric and linear structure, showing a strong paramagnetic response. The fact that the remanent magnetization and coercive field are almost negligible indicates that the system does not retain a magnetic memory, and the magnetic moments are aligned solely in response to the applied field.

Both the M_{max} value and the dM/dH slope (χ) are larger for sample C compared to sample B. This may suggest that increasing the Pr doping results in a slight increase in the number of paramagnetic centers in the system or a more effective spin alignment. These observations also support the findings of Curie-type behavior and low effective magnetic moment obtained from temperature-dependent $\chi(T)$ analyses.

Sample D, shown in Fig. 3c, exhibits classical paramagnetic behavior, similar to other Pr-doped Bi-2212 samples. However, the very shallow slope of the $M-H$ curve and the very low maximum magnetization (0.05 emu/g) indicate that the magnetic moments are further suppressed with the increase of the doping ratio.

This low susceptibility is also consistent with the low Curie constant and effective magnetic moment values obtained previously from $M-T$ curves and inverse susceptibility analysis. As a result, sample D behaves as a weak, linear, and reversible paramagnetic system, and the suppressive effect of Pr doping on the magnetic properties becomes evident. Similar linear and reversible $M-H$ characteristics have been reported in rare-earth-doped manganites and cuprates, confirming the dominance of paramagnetic behavior without significant hysteresis or coercivity [3, 4, 10].

As a result, while the $M-H$ curves reveal that all of the samples B, C, and D exhibit paramagnetic character, it is observed that both the magnetic susceptibility (χ) and maximum magnetization (M_{max}) values decrease significantly as the Pr doping ratio increases, indicating that the doping is effective in suppressing the magnetic moments.

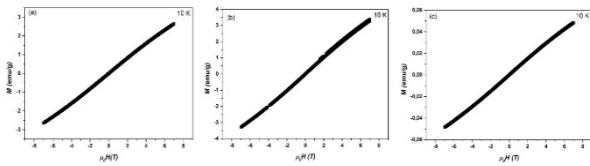


Figure 3. $M-H$ curves of samples (a) B, (b) C, and (c) D

Overall, the consistency among $\chi-T$, $1/\chi-T$, $dM/dT-T$, and $M-H$ results confirms that Pr doping systematically suppresses superconductivity while enhancing paramagnetic contributions. The next section summarizes these observations and their broader implications.

4. Conclusion

In this study, the focus was on the magnetic properties of Pr-doped $\text{Bi}_2\text{Sr}_2\text{CaCu}_2\text{O}_{8+\delta}$ (Bi-2212) ceramics, which were synthesized by the sol-gel method. The experimental program involved measuring temperature-dependent magnetization ($M-T$), reverse magnetic susceptibility ($1/\chi-T$), $dM/dT-T$ derivative curves, and $M-H$ hysteresis measurements. The samples used were B ($x = 0.1$), C ($x = 0.2$), and D ($x = 0.3$), with different Pr ratios.

Samples B, C, and D exhibited distinct paramagnetic behaviors, as evidenced by analyses performed following the Curie-Weiss

law. The calculated Curie constants for these samples were determined to be 1.11×10^{-4} emu K/cm^3 Oe, 1.07×10^{-4} emu K/cm^3 Oe, and 1.03×10^{-4} emu K/cm^3 Oe, respectively. The values thus obtained indicate a gradual decrease in the magnetic polarizability of the materials as the Pr doping ratio increases.

The Curie-Weiss temperature (θ_{CW}) was determined to be 53.85 K, 50.21 K, and 44.65 K for samples B, C, and D, respectively. These positive values indicate the predominance of short-range ferromagnetic interactions in the doped samples. This finding suggests a positive correlation between magnetic moment carrier centers, particularly at low temperatures.

The $dM/dT-T$ derivative curves demonstrated that the magnetic transitions shifted along the temperature axis, contingent on the doping ratio, and became more damped. This finding suggests that Pr doping compromises the spin ordering and affects the magnetic homogeneity of the system.

In the evaluation of $M-H$ curves, it was observed that both the saturation magnetization and magnetization cycle weakened with increasing doping rates. This finding suggests that Pr ions contribute to spin dilution within the system, thereby suppressing the magnetization that forms under the influence of the magnetic field.

It was determined that the paramagnetic nature of Bi-2212 ceramics became more pronounced as the Pr doping ratio increased.

The magnetic characterization carried out in this study provides valuable insights for engineering applications that require precise control of magnetic and electronic states. Understanding the transition from superconductivity to paramagnetism in Pr-doped Bi-2212 systems is particularly relevant for the development of spintronic materials, magnetic sensors, and low-temperature functional devices. The tunability of magnetic response through rare-earth substitution makes these materials promising candidates for future multifunctional electronic systems.

Consequently, parameters such as the Curie constant, effective magnetic moment, and Curie-

Weiss temperature underwent systematic alteration. These results indicate that Pr doping plays a significant regulatory role in magnetic behavior and that these materials have potential applications in spintronics, sensors, and low-temperature devices.

Article Information Form

Funding

This work was supported by the Research Fund of Hakkari University, Hakkari, Türkiye, under the project number FM22LTP2.

Author Contributions

Hasan Ağıl: Investigation, Methodology, Writing, Project administration. Hicran Kurt: Methodology, Analysis. Hakan Gündoğmuş: Writing – review & editing, Project consultancy.

The Declaration of Conflict of Interest/ Common Interest

Authors declare that they have no known competing financial interests or personal relationships that could have appeared to influence the work reported in this paper.

Artificial Intelligence Statement

No artificial intelligence tools were used while writing this article.

Copyright Statement

Authors own the copyright of their work published in the journal and their work is published under the CC BY-NC 4.0 license.

References

- [1] M. A. Subramanian, et al., "A new high-temperature superconductor: $\text{Bi}_2\text{Sr}_{3-x}\text{Ca}_x\text{Cu}_2\text{O}_{8+y}$ ", *Science*, vol. 239, no. 4843, pp. 1015-1017, Feb 1988. doi: 10.1126/science.239.4843.1015. [Online]. Available: <https://www.science.org/doi/10.1126/science.239.4843.1015>
- [2] P. Lee, et al., "Anomalous scattering study of the bi distribution in the 2212 superconductor: Implications for Cu valency," *Science*, vol. 244, no. 4900, pp. 62-63, Apr 1989. [Online]. Available: <https://www.science.org/doi/10.1126/science.244.4900.62>
- [3] A. Mleiki, S. Othmani, W. Cheikhrouhou-Koubaa, M. Koubaa, A. Cheikhrouhou, and E. K. Hlil, "Effect of praseodymium doping on the structural, magnetic and magnetocaloric properties of $\text{Sm}_{0.55}\text{Sr}_{0.45}\text{MnO}_3$ manganite", *Solid State Commun.*, vol. 223, pp. 6-11, Dec 2015. doi: 10.1016/j.ssc.2015.08.019. [Online]. Available: <https://doi.org/10.1016/j.ssc.2015.08.019>
- [4] K. Belala, A. Galluzzi, M. F. Mosbah, and M. Polichetti, "Transport and magnetic properties of $\text{Bi}(\text{Pb})_{2212}$ superconducting ceramics doped by low rate of potassium," *Mater. Sci.-Pol.*, vol. 39, no. 1, pp. 15-23, June 2021. doi: 10.2478/msp-2021-0005. [Online]. Available: <https://doi.org/10.2478/msp-2021-0005>
- [5] X. Sun, X. Zhao, W. Wu, X. Fan, X. – G. Li, and H. C. Ku, "Pr-doping effect on the structure and superconductivity of $\text{Bi}_2\text{Sr}_2\text{Ca}_{1-x}\text{Pr}_x\text{Cu}_2\text{O}_y$ single crystals", *Physica C*, vol. 307, no. 1–2, pp. 67-73, Oct. 1998. doi: 10.1016/S0921-4534(98)00413-4. [Online]. Available: [https://doi.org/10.1016/S0921-4534\(98\)00413-4](https://doi.org/10.1016/S0921-4534(98)00413-4)
- [6] Y. Takano, K. Morita, H. Ozaki, and K. Sekizawa, "Superconductivity and magnetism of $\text{Bi}_2\text{Sr}_2\text{Ca}_{1-x}\text{Pr}_x\text{Cu}_2\text{O}_y$ system", *J. Magn. Magn. Mater.*, vol. 140–144, no. 2, pp. 1343-1344, Feb 1995. doi: 10.1016/0304-8853(94)00664-4. [Online]. Available: [https://doi.org/10.1016/0304-8853\(94\)00664-4](https://doi.org/10.1016/0304-8853(94)00664-4)
- [7] Y. Ando, et al., "Resistive upper critical fields and irreversibility lines of optimally doped high- T_c cuprates", *Phys. Rev. B*, vol. 60, no. 17, pp. 12475-12479, Nov 1999. doi: 10.1103/PhysRevB.60.12475. [Online]. Available: <https://doi.org/10.1103/PhysRevB.60.12475>

- [8] L. Li, Y. Wang, S. Komiya, S. Ono, Y. Ando, G. D. Gu, and N. P. Ong, "Diamagnetism and Cooper pairing above T_c in cuprates," *Phys. Rev. B*, vol. 81, p. 054510, Feb. 2010. doi: 10.1103/PhysRevB.81.054510. [Online]. Available: <https://doi.org/10.1103/PhysRevB.81.054510>
- [9] H. Salamati, P. Kameli, and F. S. Razavi, "Effect of Pr doping on the superconductivity and interlayer coupling of the $\text{Bi}_2\text{Sr}_{2-x}\text{Pr}_x\text{Ca}_1\text{Cu}_2\text{O}_y$ system", *Supercond. Sci. Technol.*, vol. 16, no. 8, pp. 922-925, July 2003. doi: 10.1088/0953-2048/16/8/316. [Online]. Available: <https://doi.org/10.1088/0953-2048/16/8/316>
- [10] S. Horii, et al., "Magnetic orientation and magnetic anisotropy in paramagnetic layered oxides containing rare-earth ions", *Sci. Technol. Adv. Mater.*, vol. 10, no. 1, p. 014604, May 2009. doi: 10.1088/1468-6996/10/1/014604. [Online]. Available: <https://doi.org/10.1088/1468-6996/10/1/014604>
- [11] M. R. Koblishka, L. Püst, C.-S. Chang, T. Hauet, and A. Koblishka-Veneva, "The paramagnetic meissner effect (PME) in metallic superconductors," *Metals*, vol. 13, no. 6, p. 1140, June 2023. doi: 10.3390/met13061140. [Online]. Available: <https://doi.org/10.3390/met13061140>
- [12] K. B. Lyons, P. A. Fleury, J. P. Remeika, A. S. Cooper, and T. J. Negrán, "Dynamics of spin fluctuations in lanthanum cuprate," *Phys. Rev. B*, vol. 37, no. 4, pp. 2353-2356, Feb 1988. doi: 10.1103/PhysRevB.37.2353. [Online]. Available: <https://doi.org/10.1103/PhysRevB.37.2353>
- [13] J. L. Tallon, C. Bernhard, H. Shaked, R. L. Hitterman, and J. D. Jorgensen, "Generic superconducting phase behavior in high- T_c cuprates: T_c variation with hole concentration in $\text{YBa}_2\text{Cu}_3\text{O}_{7-\delta}$ ", *Phys. Rev. B*, vol. 51, no. 1, pp. 12911-12914, May 1995. doi: 10.1103/PhysRevB.51.12911. [Online]. Available: <https://doi.org/10.1103/PhysRevB.51.12911>
- [14] J. R. Hook and H. E. Hall, *Solid State Physics*. New York, NY, USA: Wiley, 2010.
- [15] M. Tinkham, *Introduction to Superconductivity*, 2nd ed. New York, NY, USA: McGraw-Hill, 1996.